PAPER • **OPEN ACCESS**

Combined Experimental and Numerical Approach for the Thermal Heat Exchange Investigation of Li-Ion Cells for Automotive Applications

Combined Experimental and Numerical Approach for the Thermal Heat Exchange Investigation of Li-Ion Cells for Automotive Applications

C. Karaca*[1], G. Baldinelli[1], L. Postrioti[1], F. Scrucca[2]

[1] 1 Department of Engineering - University of Perugia, Italy
[2] Department of Sustainability, ENEA - Italian National Agency for New Technologies, Energy and Sustainable Economic Development, Rome, Italy

* Corresponding author: cem.karaca@studenti.unipg.it

Abstract. Lithium-ion (Li-ion) battery is an advanced technology in the field of electrochemical energy storage, but its management constitutes one of the most intriguing challenges for electric vehicles. Many parameters need to be controlled and managed and many aspects need to be optimised. This work presents a methodology for laboratory characterization of Nickel Manganese Cobalt (NMC) Lithium-Ion batteries suited for automotive applications. The purpose consists of obtaining a detailed description of the electrical and thermal behaviour of a single battery cell to provide an accurate model (static, dynamic, and thermal) that could ensure optimized real-time battery management by a management system for several battery packs. A battery testing system was built using a bidirectional power supply and a software/hardware interface was implemented within the National Instruments LabVIEW environment that monitors current, voltage and temperature sensors. This dedicated laboratory equipment can be used to apply and report charging/discharging cycles according to the user-defined load profile. A bidimensional CFD dynamic condition/transient simulation in the Ansys FLUENT environment was performed to study the heat thermal fluxes generated by a determined current value in the battery cells, and the results have been compared to the experimental data for validation.

1. Introduction

Reduction of carbon dioxide emission is currently a main driving force to find sustainable and more efficient alternatives, rather than the traditional Internal Combustion Engines based on fossil fuels [1]. In this context, Electric Vehicles are quite promising and commercially feasible. The main difference between an Internal Combustion Engine Vehicle (ICEV) and an EV or HEV is the presence of a battery pack used to power the vehicle, where single cells are connected in series to increase the voltage, and in parallel to increase the capacity. Batteries are also the main limitation in electric vehicle spread due to their limited capacity and long charging time, lifetime, cost, and safety issues such as thermal runaway [2]. Furthermore, lithium-ion batteries have limited operating conditions restricted by temperature and voltage windows, due to performance and safety issues [3].

Therefore, it is crucial to monitor multiple parameters, such as the state of charge (SOC), temperature, load current, and to understand how battery cells would behave in certain applications. This is accomplished by implementing an electronic unit called Battery Management System (BMS).

A battery management system is a system control unit that reacts with external and internal events to safeguard the battery. It balances the cell voltage (i.e. keeping the cells at the same SOC level), overviews aging issues, and also takes corrective measures against any abnormal condition at the system infrastructure. To execute these tasks effectively, an accurate battery model, able to estimate and communicate its energy and power availability to the rest of the system from its terminal voltage and load-current history, must be implemented in the BMS online control strategy [3]. Thus, finding a fine method to characterize battery cell behaviors is useful in performance modeling and predicting degradation. For this purpose, BMS needs two essential parameters: the State of Charge (SoC) and the State of Health (SoH) [4,5].

Many studies have been released to explain the thermal conditions on batteries under different C rates and charge or discharge duration by comparing the results of CFD and experimental tests. Ö. Ekici et al. have been established their studies with the conditions as galvanostatic charge and discharge tests at 0.5C, 1.0C and 1.5C rates were conducted. Test durations were 30, 60 and 90 min, depending on the C rate values. Experiments were performed at three different operating temperatures, namely, 20°C, 35°C and 50°C [11]. Another study is a zero-dimensional numerical model based on the transient energy balances and the analogy between heat transfer and electrical transfer using resistances and capacitors. The simulations were carried at 3C discharging/0.5C charging rates and the obtained results were compared with both three-dimensional computational fluid dynamic (CFD) results and experimental results from the literature [12]. The Nickel Manganese Cobalt (NMC) lithium-ion battery cells characterization follows these steps: static characterization, dynamic characterization, and thermal characterization which are studied by a Capacity test, a Hybrid pulse power characterization test (HPPC), CFD simulations and their experimental validation.

In brief, the first test is performed since, even if a nominal capacity value is always provided by the manufacturer inside the battery cell datasheet (2.9 Ah in this case), this represents a worst-case estimate, therefore a test should be performed to estimate a more reasonable value to be employed inside the cell model. HPPC allows the proper characterization of the Electrical Equivalent Circuit (EEC) model by soliciting the battery with charging/discharging current pulses while observing its voltage response. The purpose is to define the impedance and its non-linear behavior depending on operating conditions [6] [7]. Finally, CFD simulations have been implemented to provide information about the external temperature of the cells as a function of the current values and how natural convection develops in the surrounding environment.

2. The Experimental Set-up

In this chapter we will introduce the experimental set-up used in this study. The test bench used was designed to ensure adequate data acquisition in safety, with the aim of maintaining a stable ambient temperature. The study, for reasons of statistical reliability, was conducted on 4 Li-ion cells electrically connected in parallel, NMC type and model N18650CL-29 of the company Zhengzhou BAK Battery Co., Ltd. This cell has a nominal voltage of 3.6 V, nominal capacity 2.9 Ah, with an internal impedance declared by the manufacturer ≤ 35 mΩ, and an energy density (at 1C) of 213 Wh/kg. These 4 cells have been arranged on a base designed to guarantee heat exchange with the air and avoid overheating. Figure 1 shows the batteries, the complete bench and the ITECH Battery Test System.

The cells' supports have been fixed on a wooden base, so as to ensure adequate electrical insulation. This base was closed with three walls of polystyrene, to ensure a stable temperature, and the fourth in plexiglass to ensure optical access. As it is possible to see, placed on a lower shelf, there is the entire data acquisition system including four K thermocouples to monitor the cell temperature, a PT100 thermocouple for the ambient temperature, four LEM current sensors – CTSR 1-P (characterized by a working range equal to +/- 1 A) and four LEM – CTSR 6-NP (characterized by a working range equal to +/- 6 A). For each cell there is one of these two different types of current sensors, so as to guarantee the acquisition accuracy for different current ranges.

Figure 1. Test cells, complete bench and battery cycler.

These eight current sensors were first calibrated with a NI-Virtual Bench multimeter in the effective working range, and then managed by three acquisition cards, all then connected to a PC, and they are: the NI-USB 6001 which acquires voltage data, the NI-PCI-6221 which acquires current values, and the NI-USB-6008 for temperatures. The PC also communicates with the ITECH ITS 5300 "cycler" (e.g the system capable of absorbing/receiving current from the cells connected to it in parallel) via ITECH proprietary software. The ITECH battery test system consists of two IT-6015C bidirectional power supplies (with full scale 80 V and 360 A for one, and 500 V and 90 A for the other) [8]. The wiring diagram that summarizes this configuration can be seen in Figure 2:

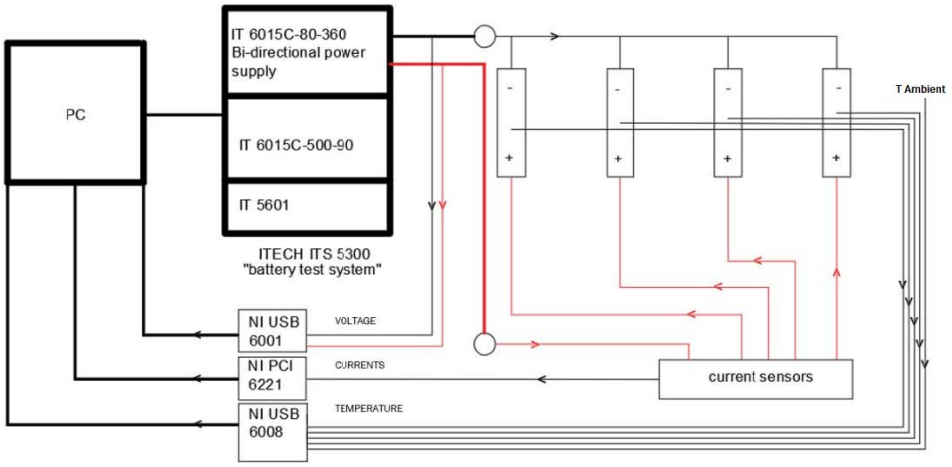

Figure 2. Wiring diagram of the test bench [8]

The management of the hardware used in the counter is entrusted to two control and acquisition systems. Respectively one, created internally in the LabVIEW environment, dedicated to data acquisition (currents, voltages and temperatures), the other implemented by ITECH which manages the charge and discharge cycles.

3. Implementation of the numerical model for the computational approach

CFD simulations are implemented by Ansys Fluent for thermal conditions and thermal exchange between cells and air. This part examines each step of simulation from creation of geometry to results of analysis (Figure 3).

As software, Solidworks and Autocad are used to design geometry of the simulation. Firstly, 3D test bench model is divided in four equal parts with the same conditions in the test bench. Only 2 batteries and air domain remain in the final 3D model.

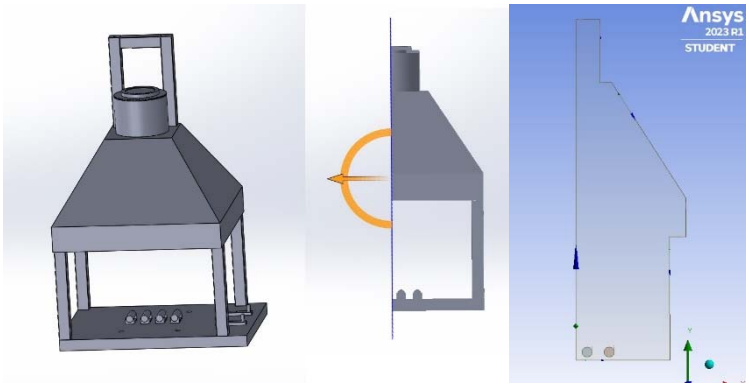

Figure 3. 3D Geometry created by Solidworks and 2D Geometry

Secondly, the 3D geometry is converted to a 2D geometry and imported to Ansys Workbench. The Fluent module is used to see the energy exchange between cells and air domain. “Mesh inflation” is applied inside (three layers) and outside (seven layers) of the cells and generated “First layer thickness”, which equals 0.0005m. Triangular type mesh is selected for all the model. Symmetry edge, insulated edge, bottom, cap edges are applied. A total of 68,891 elements are generated after all these meshing selection.

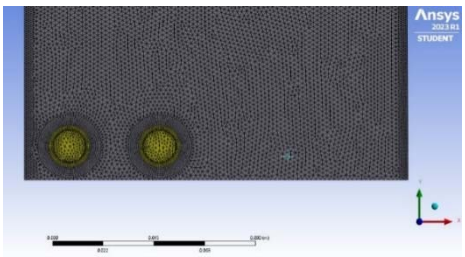

Figure 4. Meshing condition in batteries, air domain and walls

The next step for the CFD simulation is the Fluent-Setup section. Simulation conditions have been defined according to experimental test conditions. First of all, transient conditions are selected with 49 time steps. Each time step lasts 60 seconds with a maximum of 1,300 iteration. The chosen viscous model is “Laminar”, pressure based conditions; gravity is obviously applied. Discharge is simulated in 2.75 A (C rate) for one cell. Each cell has 35 $m\Omega$ nominal internal resistance (assumed as measured in ambient temperature conditions, at SOC 100%), 2,360 $kg/m3$ density, 1,000 J/kgK specific heat and 1 W/mK thermal conductivity.

A.H. Mahmud *at al.* issued a study on the impact of SOC and temperature on internal resistance of Li-ion cells. Based on their research results, the battery internal resistance typically evidences a significant decrease with temperature, around 70 % for cells going from 10°C to 35 °C [12]. Considering the relevance of the energy source intensity for the thermal evolution of the cells, in our simulation the internal resistance has been supposed to assume different values, calculated accordingly the SoC values evaluated during the discharging phase. The assumed internal resistance vs. the SoC trend is shown in Figure 6.

The duration of the simulation steps in which different values of internal resistance are assumed have been selected after monitoring the SOC of batteries during the experimental test. Experimental test results gave the state of charge for each battery with the discharge duration. Figure 6 shows the voltage values vs. SOC percentage. Other researchers evidenced how the internal resistance as a function of SoC for Li-ion cells can have significantly different trends. In particular, in [9] experimental test results highlighted how that internal resistance was at maximum value when the battery capacity was empty.

The minimum value of the internal resistance was not noticeable at the time at 100% SOC, but at a point between 80% and 90%. Four batteries are used in their research and the results are shown as Figure 7. As it will be shown in the following section, assuming different trends for internal resistance can have dramatic effects on the cell temperature time-history.

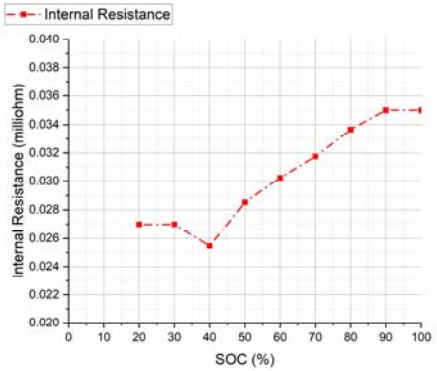

Figure 5. Internal resistance of test batteries vs. SoC, from [12]

% SoC	Voltage (V)
0	2.841
2.5	2.874
5	2.907
10	2.974
20	3.107
30	3.24
40	3.374
50	3.507
60	3.64
70	3.774
80	3.907
90	4.04
95	4.106
100	4.174

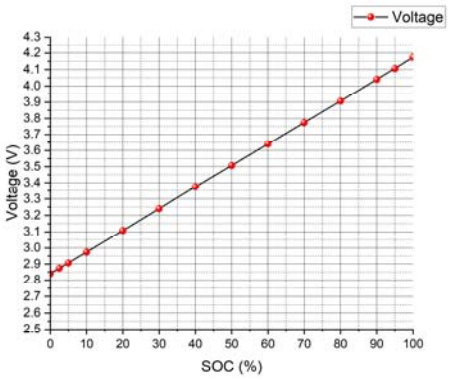

Figure 6. Voltage values which equals to SoC percentage

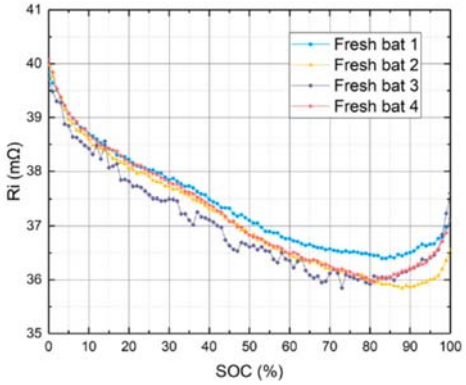

Figure 7. R_i-SOC plot for different batteries [9]

4. Experimental Test and Results

After the preparation of the experimental setup, the capacity test is started with the steps reported in Figure 8, while the test evolution is reported in Figure 9.

As can be seen in Figure 9, In step 1, the cell is simply following the ambient temperature evolution.

In step 2, a C/20 moderate current is flowing hence the cell temperature gradient is slightly increased in the first 2 hours in step 2. Later a moderate temperature increase is observed and then cells slowly

reach a thermal equilibrium with ambient temperature; equilibrium is achieved about at time 40k seconds. Step 3 starts from a thermal equilibrium condition and immediately the temperature starts raising with a significand gradient due to intense current (1C rate discharge). In step 3, the temperature gradient follows the resistance trend in fig 6 i.e. the initial temperature gradient is higher, for higher resistance; as the cell is discharged, the gradient is progressively reduced.

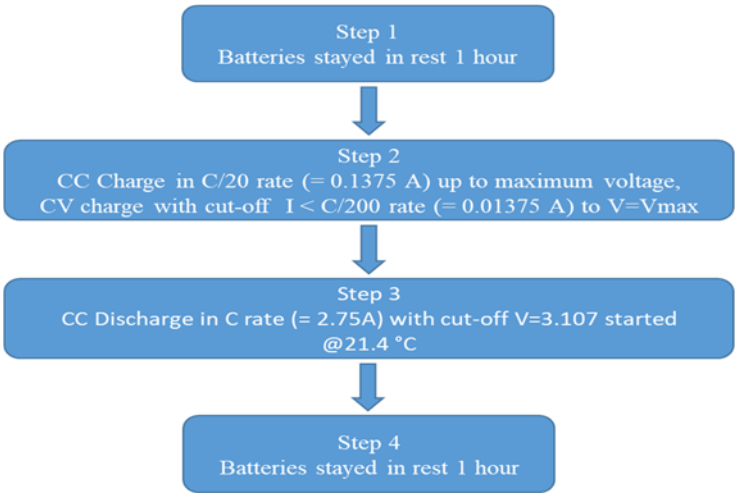

Figure 8. Sequence of the experimental setup steps

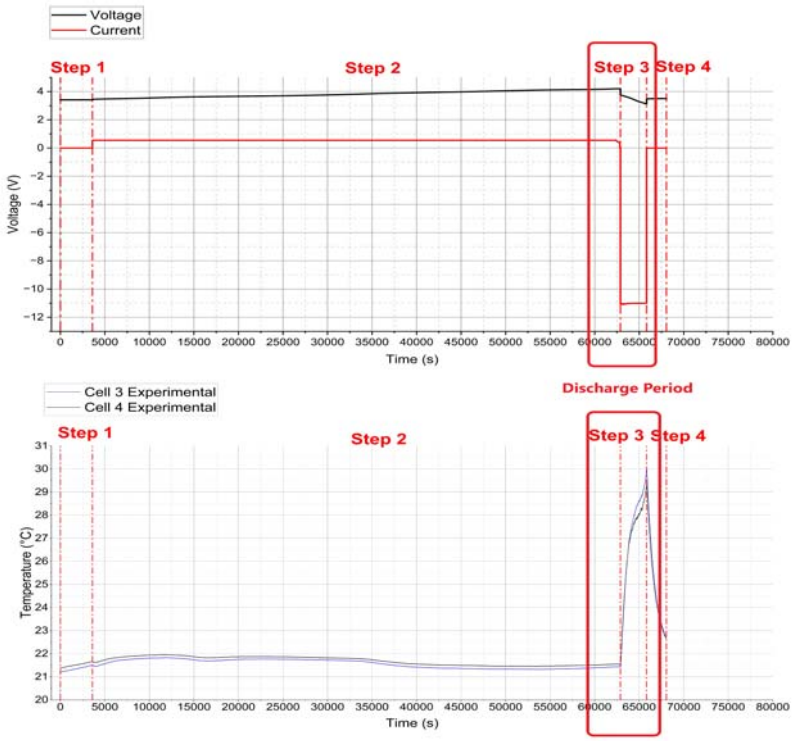

Figure 9. Capacity Test Voltage/Current-Time Graph and Cells-Temperature Graph

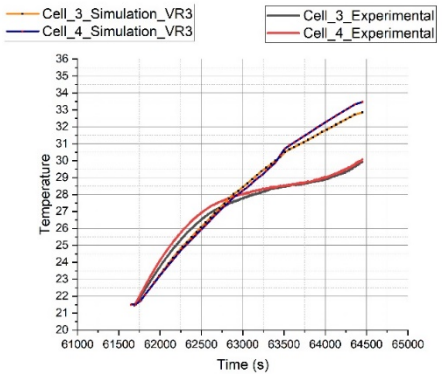

Figure 10. Comparison of experimental test and CFD simulation VR3 vs time.

Voltage and current values are shown in the top graph of Figure 9 during the charge and discharge conditions. Also each step is divided with red dash-dot lines. Current value is 0 during the resting time but OCV is 3.435V in the first step. In the second step, constant current is 0.55 A (for the 4 batteries). This section provides to the batteries to reach to maximum voltage level which is defined by manufacturer as 4.20V. After all batteries are fully charged, discharging duration is started in the step three. The discharge is applied with a constant current, -11 A for the 4 batteries to reach the OCV of batteries of 3.107 V. The discharging period goes for each battery from 100% of SoC to 20%. The resting period followed the discharging period and the resting time is 1 hour in the step four.

The comparison between tests and simulations are shown in Figure 10. Cell 3 and Cell 4 temperature time-profile are sketched during the discharge period, varying the resistance according to the assumption reported in Figure 5. Simulation_VR3 is run assuming seven different internal resistances values for each cell as the SoC was progressively decreased during the CC discharge Step 3. The temperatures of simulation results are almost 4 °C higher than the experimental ones.

In Simulation_VR2, the internal resistance *vs.* SoC dependence was assumed to be different, using three different internal resistance values. These internal resistances are 35 mΩ, 17.5 mΩ and 22.5 mΩ. The temperature time-profile resulting from Simulation_VR2 are reported in Figure 11; as can be seen, with this assumption of the temperature trend, the simulations are in very good agreement with the experimental data.

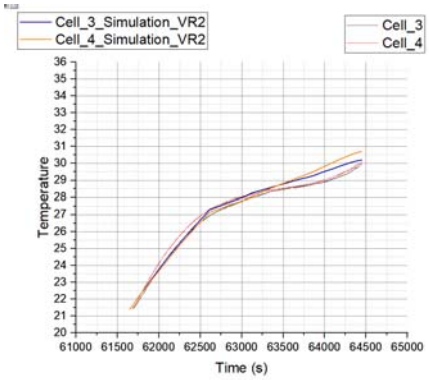

Figure 11. Comparison of experimental test and CFD simulation VR2 vs time.

5. Conclusions

In the present activity, an experimental test bench for the analysis of thermal behaviour of four Li-ion batteries was developed by using the NI-USB 6001 which acquires voltage data, the NI-PCI-6221 which acquires current values, the NI-USB-6008 for temperatures and the ITECH ITS 5300 which has battery test system consists of two IT-6015C bidirectional power supplies. Applied 4 steps are resting, CC-CV

charging, CC discharging and finally resting step again, have been set. Batteries thermal condition are monitored, between from 100% SoC to 20% SoC of batteries, during only step 3 which is CC discharging.

A numerical methodology for the CFD simulation of thermal evolution of cells, thermal fields and thermal exchange with surrounding air. CFD simulation is run as 2D analysing. 2 cells, surrounding air and boundary conditions have been defined respecting to the experimental test conditions. Also in the simulation, only step 3, CC discharging, is analysed.

The relevant influence of internal resistance dependence on SoC was proved, with different assumptions resulting in significantly different thermal evolution of cells. Internal resistance is related to temperature, SoC and discharge rate and any changes of temperature, SoC or discharge rate can impact the value of internal resistance [10]. The study shows that internal resistance can be decrease almost half values in the different SoC but when it reaches minimum degree, it doesn't increase reasonable during the discharging.

6. References

[1] V. Ruiz, A. Pfrang, A. Kriston, N. Omar, P. van den Bossche, and L. Boon-Brett, "A review of international abuse testing standards and regulations for lithium-ion batteries in electric and hybrid electric vehicles," *Renewable and Sustainable Energy Reviews*, vol. **81**. Elsevier Ltd, pp. 1427–1452, Jan. 01, 2018. DOI: 10.1016/j.rser.2017.05.195.

[2] E. Vergori, F. Mocera, and A. Somà, "Battery modeling and simulation using a programmable testing equipment," *Computers*, vol. **7**, no. 2, 2018, DOI: 10.3390/computers7020020

[3] H. A. Gabbar, A. M. Othman, and M. R. Abdussami, "Review of Battery Management Systems (BMS) Development and Industrial Standards," *Technologies*, vol. **9**, no. 2, p. 28, Apr. 2021, DOI: 10.3390/technologies9020028.

[4] S. Singirikonda and Y. P. Obulesu, "Advanced SOC and SOH Estimation Methods for EV Batteries—A Review," in *Lecture Notes in Electrical Engineering*, 2021, vol. 700, pp. 1963–1977. DOI: 10.1007/978-981-15-8221-9_182.

[5] M. Thingvad, L. Calearo, A. Thingvad, R. Viskinde, and M. Marinelli, "Characterization of NMC Lithium-ion Battery Degradation for Improved Online State Estimation," Sep. 2020. DOI: 10.1109/UPEC49904.2020.9209879.

[6] D. Cittanti, A. Ferraris, A. Airale, S. Fiorot, S. Scavuzzo, and M. Carello, "Modeling Li-ion batteries for automotive application: A trade-off between accuracy and complexity," 2017. DOI: 10.23919/EETA.2017.7993213.

[7] D. I. Stroe, M. Swierczynski, A. I. Stroe, and S. K. Kær, "Generalized characterization methodology for performance modeling of lithium-ion batteries," *Batteries*, vol. **2**, no. 4, Dec. 2016, DOI: 10.3390/batteries2040037.

[8] E. Valentini, L. Postrioti, G. Baldinelli, "Analisi Sperimentale Delle Caratteristiche Elettriche E Di Scambio Termico Di Celle Li-Ion Per Impiego Automotive,"2022, Master Thesis, Perugia University.

[9] D. Wang, Y. Bao, J. Shi, "Online Lithium-Ion Battery Internal Resistance Measurement Application in State-of-Charge Estimation Using the Extended Kalman Filter," 2017, *Energy MDPI*, Basel, Switzerland.

[10] L. Chen, M. Zhang, Y. Ding, S. Wu, Y. Li, G. Liang, H. Li, H. Pan, "Estimation the internal resistance of lithium-ion-battery using a multi-factor dynamic internal resistance model with an error compensation strategy", 2021, *Electrochem. SoC*. Interface 21-61, Volume **7**, Pages 3050-3059.

[11] A. Amini, Ö. Ekici, T. Özdemir, S. Ç. Başlamışlı, M. Köksal, "A thermal model for Li-ion batteries operating under dynamic conditions", 2021, *Applied Thermal Engineering*, Vol **185**

[12] A.H. Mahmud, Z. H. C. Daud, Z. Asus, "The Impact Of Battery Operating Temperature And State Of Charge On The Lithium-Ion Battery Internal Resistance", 2017, *Jurnal Mekanikal*, Vol **40**, 01-08